Published as: *J Struct Biol*. 2011 April ; 174(1): 239–244.

Crystal structure of a hemojuvelin-binding fragment of neogenin at 1.8 Å

Fan Yang[a,b], **Anthony P. West Jr.**[b], and **Pamela J. Bjorkman**[b,c,*]

[a]Graduate option in Chemistry and Chemical Engineering, California Institute of Technology, Pasadena, California 91125

[b]Division of Biology, California Institute of Technology, Pasadena, California 91125

[c]Howard Hughes Medical Institute, California Institute of Technology, Pasadena, California 91125

Abstract

Neogenin is a type I transmembrane glycoprotein with a large ectodomain containing tandem immunoglobulin-like and fibronectin type III (FNIII) domains. Closely related to the tumor suppressor gene DCC, neogenin functions in critical biological processes through binding to various ligands, including netrin, repulsive guidance molecules, and the iron regulatory protein hemojuvelin. We previously reported that neogenin binds to hemojuvelin through its membrane-proximal fifth and sixth FNIII domains (FN5-6), with domain 6 (FN6) contributing the majority of critical binding interactions. Here we present the crystal structure of FN5-6, the hemojuvelin-binding fragment of human neogenin, at 1.8 Å. The two FNIII domains are orientated nearly linearly, a domain arrangement most similar to that of a tandem FNIII-containing fragment within the cytoplasmic tail of the β4 integrin. By mapping surface-exposed residues that differ between neogenin FN5-6 and the comparable domains from DCC, which does not bind hemojuvelin, we identified a potential hemojuvelin binding site on neogenin FN6. Neogenin FN5, which does not bind hemojuvelin in isolation, exhibits a highly electropositive surface, which may be involved in interactions with negatively-charged polysaccharides or phospholipids in the membrane bilayer. The neogenin FN5-6 structure can be used to facilitate a molecular understanding of neogenin's interaction with hemojuvelin to regulate iron homeostasis and with hemojuvelin-related repulsive guidance molecules to mediate axon guidance.

Keywords

neogenin; hemojuvelin; crystal structure; FNIII domain; iron homeostasis; repulsive guidance molecule

1. Introduction

Neogenin is a type I transmembrane glycoprotein expressed in multiple tissues including brain, kidney, liver, and skeletal muscle (Meyerhardt et al., 1997; Vielmetter et al., 1997). Closely-related to the tumor suppressor molecule DCC (Deleted in Colorectal Cancer) (Vielmetter et al., 1994), neogenin is composed of four immunoglobulin (Ig)-like domains followed by six fibronectin type III (FNIII) domains, a transmembrane region, and a

*To whom correspondence should be addressed: Division of Biology, California Institute of Technology, 1200 E. California Blvd. MC 114-96, Pasadena, CA. Tel.: 626-395-8350; Fax: 626-792-3693; bjorkman@caltech.edu.

Protein Data Bank accession code Coordinates and structure factors for neogenin FN5-6 have been deposited with RCSB Protein Data Bank with code 3P4L.

cytoplasmic domain (Vielmetter et al., 1994; Vielmetter et al., 1997). Neogenin functions in a variety of developmental and metabolic processes (Wilson and Key, 2007), and several ligands have been identified, including netrin, repulsive guidance molecules (RGMs) (Matsunaga and Chedotal, 2004; Matsunaga et al., 2004; Rajagopalan et al., 2004), and the iron regulatory protein hemojuvelin (Zhang et al., 2005).

While netrin-1 and neogenin mediate chemoattractive axon guidance, the neogenin/RGMa interaction functions specifically in axon repulsion (Wilson and Key, 2006). Neogenin has also been implicated as a dependence receptor (Bredesen et al., 2005), such that it triggers apoptosis in the absence of a ligand RGM molecule, whereas the ligand-bound state inhibits this effect (Matsunaga and Chedotal, 2004; Matsunaga et al., 2004). Downstream signaling elicited by the binding of neogenin to RGMa involves the Rho family of small GTP-binding proteins, which regulate cytoskeletal dynamics by controlling actin filaments and causing growth cone collapse (Conrad et al., 2007). Pre-incubation of netrin-1 inhibits this signaling, indicating either that netrin-1 occludes the RGMa-binding site on neogenin, or that a different signaling cascade is initiated to counteract the Rho-mediated signaling (Conrad et al., 2007).

In hepatocytes and perhaps also skeletal muscle, neogenin is involved in iron homeostasis through interactions with hemojuvelin, also known as HFE2 or RGMc (Zhang et al., 2005). Hemojuvelin is a glycosylphosphatidylinositol (GPI)-anchored protein that shares sequence similarity with RGMa and RGMb, which, unlike hemojuvelin (RGMc), are expressed predominantly in the nervous system (Schmidtmer and Engelkamp, 2004). Hemojuvelin is an upstream modulator of hepcidin, a peptide hormone that regulates iron flux in mammals (Lin et al., 2005). Interaction with neogenin has been suggested to initiate retrograde trafficking of membrane-bound hemojuvelin to the Golgi and trans-Golgi network for further processing before soluble hemojuvelin is released from the cell (Maxson et al., 2009; Zhang et al., 2007; Zhang et al., 2008). The ratio of membrane-bound and soluble forms of hemojuvelin is believed to be important for determining the amount of signal sent to the nucleus through the bone morphogenetic protein (BMP)/hemojuvelin pathway, which regulates hepcidin expression levels (Babitt et al., 2006).

We previously described biochemical studies using neogenin ectodomain deletion mutants to localize the hemojuvelin-binding site to the two membrane-proximal FNIII domains (FN5-6) (Yang et al., 2008). The FN5-6 fragment was as effective as the intact neogenin ectodomain in competing with cell membrane neogenin both *in vitro* (Zhang et al., 2008) and *in vivo* (Zhang et al., 2009), suggesting that the FN5-6 region contains the hemojuvelin-binding region on neogenin. While FN5 did not bind detectably to hemojuvelin, FN6 alone bound hemojuvelin, although more weakly than FN5-6, suggesting a potential contribution from the domain linking region in the binding interaction (Yang et al., 2008).

Here we report the crystal structure of the hemojuvelin-binding fragment of human neogenin, FN5-6, at 1.8 Å resolution. Each domain adopts the canonical FNIII fold, with the two domains arranged nearly linearly, surprisingly similar to the arrangement of a pair of tandem FNIII domains from the cytoplasmic tail of the β4 integrin. The neogenin FN5 domain displays a highly positively-charged surface, a feature shared with DCC FN5 and other proteins known to bind heparan sulfate (Bennett et al., 1997; McLellan et al., 2006). In addition to the possibility of interacting with negatively-charged carbohydrate or protein ligands, we suggest that the positive surface on the neogenin FN5 domain may promote interactions with negatively-charged phospholipids to facilitate exposure of the hemojuvelin-binding FN6 domain to hemojuvelin proteins on the surface of another cell. To gain insight into which portion of neogenin FN5-6 interacts with hemojuvelin, we mapped non-conserved residues from the comparable domains of DCC, which does not bind

hemojuvelin, onto the neogenin FN5-6 structure. One side of the FN6 domain, comprising strands C, C', F, and G, contains a high concentration of non-conserved surface residues, suggesting that this face of the molecule contains the potential hemojuvelin-binding site.

2. Materials and Methods

2.1 Crystallization and data collections

Neogenin FN5-6, corresponding to the fifth and sixth FNIII domains of human neogenin (residues 853-1054) plus a C-terminal 6x-His tag, was expressed in baculovirus-infected insect cells and purified from supernatants as previously described (Yang et al., 2008). This version of neogenin FN5-6 was previously referred to as sFNIII 5-6 to distinguish it from a longer version of these domains (FNIII 5-6; residues 851-1103). The longer version bound to hemojuvelin with ~18 fold higher affinity than FN5-6 (Yang et al., 2008), but did not crystallize, presumably due to disorder of the C-terminal extension. The best crystals were obtained from FN5-6 purified from culture media supplemented with 0.5 mg/L tunicamycin (Sigma) to inhibit addition of N-linked glycans. Crystallization screening was done using a Mosquito nanoliter handling system (TTP LabTech) with drops containing 200 nL protein plus an equal volume of reservoir solution. Initial crystals grew in mother liquor containing 0.1 M Tris, pH 8.5, 0.2 M ammonium sulfate, 25% PEG-3350 at 20°. Larger crystals were obtained in a Qiagen 24-well screw-top hanging drop plate using the same mother liquor. A single crystal was cryo-preserved in mother liquor supplemented with 5% glycerol and a native data set was collected on an R-AXIS-VI rotating anode X-ray generator (Rigaku) at 100 K.

2.2 Structure determination and model refinement

Data were processed by Denzo and scaled using Scalepack (Otwinowski and Minor, 1997) in the orthorhombic space group $C222_1$ (a = 52.6 Å, b = 112.9 Å, c = 80.9 Å). The calculated Matthews coefficient (V_M=2.5 $Å^3$/Da) (Matthews, 1968) suggested a solvent content of 51% and one molecule per asymmetric unit. The structure was solved by molecular replacement using the program Phaser (McCoy et al., 2007) and search models derived from NMR structures of individual domains of neogenin (PDB codes 1X5J and 1X5K) in which residues not present in our construct were deleted. Solvent-flattened electron density maps for model building were generated using the program DM (CCP4, 1994). After rigid body refinement, the model was iteratively improved using cycles of refinement using CNS (Brunger et al., 1998) and manual rebuilding using COOT (Emsley and Cowtan, 2004) into $2F_o$-F_c annealed omit maps. The final model (R_{cryst}= 20.0% and R_{free} = 23.4%) consists of neogenin residues 853-899 and 903-1052 (residues 900-902 were disordered), and 293 water molecules (Table 1). For analyses of contacts and buried surface areas, FN5 was defined as residues 853-949, and FN6 was defined as residues 952-1052. The CCP4 program Areaimol (CCP4, 1994; Lee and Richards, 1971; Saff and Kuijlaars, 1997) was used to calculate buried surface area using a 1.4 Å probe and to identify interacting residues using the following criteria: a distance of <3.5 Å and a hydrogen bond angle of >90° for hydrogen bonds and a maximum distance of 4.0 Å for van der Waals interactions. Figures were prepared by Pymol (DeLano, 2002).

3. Results

3.1 Overview of the neogenin FN5-6 structure

Initial crystallization trials with insect cell-expressed neogenin FN5-6 yielded crystals that diffracted to only 15 Å. The expression of FN5-6 was repeated in the presence of tunicamycin, an inhibitor of N-linked glycosylation. Neogenin FN5-6 derived from tunicamycin-treated cells migrated as a slightly smaller apparent molecular weight than its

untreated counterpart, consistent with successful inhibition of glycan attachment to the single predicted N-linked glycosylation site in FN5-6 (data not shown), and crystals obtained from the treated protein diffracted to 1.8 Å. A molecular replacement solution was obtained by searching simultaneously for the two individual FNIII domains.

The structure of neogenin FN5-6 reveals two domains arranged in an extended conformation (Figure 1A). The neogenin FNIII domains share the canonical FNIII folding topology, with each FNIII domain containing two anti-parallel β-sheets, one formed by β-strands A, B, and E and the other by β-strands C', C, F, and G. Preceding strand G in both domains is a polyproline II helix, a common feature of FNIII domains (Huber et al., 1994). Another polyproline II helix (residue 1-5) is present in strand A in the FN5 domain and a short 3_{10} helix is found between strands C and C' in the FN6 domain. The two domains interact via a hydrogen bonding network (Figure 1B) that stabilizes the extended conformation observed for the structure in the crystals. The hydrogen bonding network, taken together with a lack of obvious crystal contacts that would promote the observed interdomain conformation, suggest that the domain arrangement in the crystals would be preserved in solution.

3.2 Comparison with other FNIII domain structures

The DaliLite server (Holm et al., 2008) was used to compare the neogenin FN5-6 structure with other FNIII domains. In isolation, the closest structural homolog of neogenin FN5 is the FN1 domain from the plectin-bound β4 integrin (de Pereda et al., 2009), and neogenin FN6 is most closely related to DCC FN6 (PDB code 2EDE; to be published). We also compared neogenin FN5-6 to available tandem FNIII structures including the β4 integrin cytoplasmic domain (de Pereda et al., 1999), neuroglian FN1-2 (Huber et al., 1994), NCAM FN1-2 (Carafoli et al., 2008), fibronectin FN7-10 (Leahy et al., 1996), NCAM2 FN1-2 (PDB code 2JLL; to be published), and Ihog FN1-2 (McLellan et al., 2006). The neogenin FN5-6 domain arrangement was most similar to the arrangement of FNIII domains in the intracellular region of the β4 integrin (Supplementary Figure 1A), both in the interdomain tilt angle and the relative rotation angle (Table 2). A total of ~500 $Å^2$ was buried between the two neogenin FNIII domains, an intermediate value for buried surface areas in tandem FNIII domain structures, which ranged from 280 Å for NCAM2 FN1-2 to 1170 Å for Ihog FN1-2.

Electrostatic potential calculations revealed that neogenin FN5 is highly positively charged (Figure 1C), a feature shared with only a few other FNIII domains with structures available in the Protein Data Bank: of 80 available structures of FNIII domains, the only highly positively-charged domains were from the FN5 domain of DCC (PDB code 2EDD; to be published) (Figure 1C), FN1 from Ihog (McLellan et al., 2006), and FNIII domains from four other unpublished structures (PDB codes 1X4Z, 1UEN, 1WFT, and 1UJT). Calculated electrostatic potential surfaces for a subset of these FNIII structures (the available tandem FNIII domain structures) are shown in Supplementary Figure 1B.

3.3 Sequence comparison with DCC molecule and implications for ligand binding

We previously showed that isolated neogenin FN6 (sFNIII 6; residues 952-1054) bound to hemojuvelin with an affinity of ~2 μM, almost 1000-fold more weakly than neogenin FN5-6, whereas isolated neogenin FN5 (sFNIII 5; residues 853-952) showed no detectable binding to hemojuvelin (Yang et al., 2008). These results suggested that the hemojuvelin-binding epitope (and by analogy, the RGM-binding epitope) on neogenin is primarily located in FN6. To gain insight into potential hemojuvelin/RGM-binding interface(s) on neogenin, we mapped residues from DCC onto the neogenin FN5-6 structure. Previous studies demonstrated that hemojuvelin does not bind DCC, although neogenin FN5-6 and DCC FN5-6 share 64% sequence identity and 83% similarity (Figure 2A) and DCC is the

closest homolog of neogenin (Zhang et al., 2005). Thus a concentration of non-conserved residues could represent a potential hemojuvelin/RGM binding interface on neogenin. A portion of FN6 comprising the 3_{10} helix in the C-C' loop, the C' strand, and the loop between strands E and F is enriched in non-conserved surface residues, suggesting its potential involvement in binding hemojuvelin (Figure 2B).

The highly positive nature of the neogenin FN5 domain (Figure 1C) suggests a model (Figure 3) in which the FN5 domain interacts with negatively-charged phospholipids on the membrane bilayer to expose the membrane-proximal FN6 domain of neogenin for trans (between cells) interactions with RGMs (Yamashita et al., 2007). Alternatively, the basic patch on FN5 could bind to an as yet unidentified highly negatively-charged protein ligand or to negatively-charged polysaccharide chains, such as heparan sulfate, as has been demonstrated for DCC FN5 (Bennett et al., 1997) and for Ihog (McLellan et al., 2006).

4. Discussion

Tandem FNIII domains are found in many signal-transducing cell surface receptors, including gp130, Ihog, neuroglian, and neogenin. Although a FNIII fold can be identified from sequence information alone, the arrangement of tandem FNIII domains cannot be predicted from a sequence. Structures of tandem FNIII domains have revealed a variety of domain arrangements, ranging from nearly linear (e.g., β4 integrin) to slightly or completely bent (e.g., NCAM, neuroglian, fibronectin, and Ihog FNIII domains) (Supplementary Figure 1A). The crystal structure of the hemojuvelin-binding neogenin FN5-6 fragment reported here reveals a nearly linear domain arrangement. Surprisingly, this arrangement is most similar to the arrangement of intracellular FNIII domains in the cytoplasmic tail of the β4 integrin. The significance of the structural similarity between tandem FNIII domains in the extracellular region of neogenin and the intracellular region of an integrin is unknown.

The neogenin FN5-6 structure revealed an unusually electropositive surface, which is shared by only a few other FNIII domains, including DCC FN5 and Ihog FN1. Both DCC FN5 and Ihog FN1 bind to heparan sulfate (Bennett et al., 1997; McLellan et al., 2006), suggesting that neogenin FN5 may also interact with heparan or other negatively-charged polysaccharide chains. Alternatively, or perhaps in addition to, binding to heparan sulfate, the positive charges on neogenin FN5 could facilitate ligand (hemojuvelin or RGM) access to the membrane-proximal FN6 domain through interactions between FN5 and negatively-charged lipids on the membrane bilayer (Figure 3). The surface of DCC FN5 is also highly positive (Figure 1C) and the basic residues in the DCC and neogenin FN5 domains are mostly conserved (Figure 2A), suggesting a similar function for DCC FN5. Consistent with this idea, the netrin-binding site on DCC has been mapped to a nearby region; either FN4 or FN5 (Geisbrecht et al., 2003; Kruger et al., 2004).

The discovery of hemojuvelin as a co-receptor for BMP during activation of hepcidin expression (Babitt et al., 2006) suggested the possibility of using BMP antagonists for the treatment of anemia (Browne and Reddan, 2009). Alternatively, since the neogenin FN5-6 fragment described here has been shown to suppress BMP-mediated hepcidin expression both in vitro and in vivo (Zhang et al., 2009), it may be possible to treat anemia by using this fragment. Identification of a potential hemojuvelin-binding site on neogenin FN6 (Figure 2B) may be informative in designing such a drug if modifications are needed.

Supplementary Material

Refer to Web version on PubMed Central for supplementary material.

Acknowledgments

We thank Inder Nangiana and the Caltech Protein Expression Center for assistance with protein expression, Pavle Nickolovski and the Caltech Molecular Observatory for assistance with automated crystallization, Dr. Leonard Thomas for help with X-ray data collection, and members of the Bjorkman lab for critical reading of the manuscript. The authors acknowledge the Gordon and Betty Moore Foundation for support of the Molecular Observatory at Caltech.

Abbreviations used

DCC	deleted in colorectal cancer
Ig	immunoglobulin
FNIII	fibronectin type III
RGM	repulsive guidance molecule
BMP	bone morphogenetic protein
Ihog	interference hedgehog

References

Babitt JL, Huang FW, Wrighting DM, Xia Y, Sidis Y, Samad TA, Campagna JA, Chung RT, Schneyer AL, Woolf CJ, Andrews NC, Lin HY. Bone morphogenetic protein signaling by hemojuvelin regulates hepcidin expression. Nat Genet. 2006; 38:531–9. [PubMed: 16604073]

Baker NA, Sept D, Joseph S, Holst MJ, McCammon JA. Electrostatics of nanosystems: application to microtubules and the ribosome. Proc Natl Acad Sci U S A. 2001; 98:10037–41. [PubMed: 11517324]

Bennett KL, Bradshaw J, Youngman T, Rodgers J, Greenfield B, Aruffo A, Linsley PS. Deleted in colorectal carcinoma (DCC) binds heparin via its fifth fibronectin type III domain. J Biol Chem. 1997; 272:26940–6. [PubMed: 9341129]

Bredesen DE, Mehlen P, Rabizadeh S. Receptors that mediate cellular dependence. Cell Death and Differentiation. 2005; 12:1031–1043. [PubMed: 16015380]

Browne SA, Reddan D. Potential role of bone morphogenetic protein (BMP) signalling as a potential therapeutic target for modification of iron balance. Nephrol Dial Transplant. 2009; 24:28–30. [PubMed: 18832439]

Brunger AT, Adams PD, Clore GM, DeLano WL, Gros P, Grosse-Kunstleve RW, Jiang JS, Kuszewski J, Nilges M, Pannu NS, Read RJ, Rice LM, Simonson T, Warren GL. Crystallography & NMR system: A new software suite for macromolecular structure determination. Acta Crystallogr D Biol Crystallogr. 1998; 54:905–21. [PubMed: 9757107]

Carafoli F, Saffell JL, Hohenester E. Structure of the tandem fibronectin type 3 domains of neural cell adhesion molecule. J Mol Biol. 2008; 377:524–34. [PubMed: 18261743]

CCP4. The CCP4 suite: programs for protein crystallography. Acta Crystallogr D Biol Crystallogr. 1994; 50:760–3. [PubMed: 15299374]

Conrad S, Genth H, Hofmann F, Just I, Skutella T. Neogenin-RGMa signaling at the growth cone is bone morphogenetic protein-independent and involves RhoA, ROCK, and PKC. Journal of Biological Chemistry. 2007; 282:16423–16433. [PubMed: 17389603]

de Pereda JM, Wiche G, Liddington RC. Crystal structure of a tandem pair of fibronectin type III domains from the cytoplasmic tail of integrin alpha 6 beta 4. Embo Journal. 1999; 18:4087–4095. [PubMed: 10428948]

de Pereda JM, Lillo MP, Sonnenberg A. Structural basis of the interaction between integrin alpha 6 beta 4 and plectin at the hemidesmosomes. Embo Journal. 2009; 28:1180–1190. [PubMed: 19242489]

DeLano, WL. The PyMOL Molecular Graphics System DeLano Scientific. San Carlos, CA: 2002.

Emsley P, Cowtan K. Coot: model-building tools for molecular graphics. Acta Crystallogr D Biol Crystallogr. 2004; 60:2126–32. [PubMed: 15572765]

Geisbrecht BV, Dowd KA, Barfield RW, Longo PA, Leahy DJ. Netrin binds discrete subdomains of DCC and UNC5 and mediates interactions between DCC and heparin. J Biol Chem. 2003; 278:32561–8. [PubMed: 12810718]

Holm L, Kaariainen S, Rosenstrom P, Schenkel A. Searching protein structure databases with DaliLite v.3. Bioinformatics. 2008; 24:2780–1. [PubMed: 18818215]

Huber AH, Wang YM, Bieber AJ, Bjorkman PJ. Crystal structure of tandem type III fibronectin domains from Drosophila neuroglian at 2.0 A. Neuron. 1994; 12:717–31. [PubMed: 7512815]

Kruger RP, Lee J, Li W, Guan KL. Mapping netrin receptor binding reveals domains of Unc5 regulating its tyrosine phosphorylation. J Neurosci. 2004; 24:10826–34. [PubMed: 15574733]

Leahy DJ, Aukhil I, Erickson HP. 2.0 A crystal structure of a four-domain segment of human fibronectin encompassing the RGD loop and synergy region. Cell. 1996; 84:155–64. [PubMed: 8548820]

Lee B, Richards FM. The interpretation of protein structures: estimation of static accessibility. J Mol Biol. 1971; 55:379–400. [PubMed: 5551392]

Lin L, Goldberg YP, Ganz T. Competitive regulation of hepcidin mRNA by soluble and cell-associated hemojuvelin. Blood. 2005; 106:2884–9. [PubMed: 15998830]

Matsunaga E, Chedotal A. Repulsive guidance molecule/neogenin: a novel ligand-receptor system playing multiple roles in neural development. Dev Growth Differ. 2004; 46:481–6. [PubMed: 15610137]

Matsunaga E, Tauszig-Delamasure S, Monnier PP, Mueller BK, Strittmatter SM, Mehlen P, Chedotal A. RGM and its receptor neogenin regulate neuronal survival. Nat Cell Biol. 2004; 6:749–55. [PubMed: 15258591]

Matthews BW. Solvent content of protein crystals. J Mol Biol. 1968; 33:491–7. [PubMed: 5700707]

Maxson JE, Enns CA, Zhang AS. Processing of hemojuvelin requires retrograde trafficking to the Golgi in HepG2 cells. Blood. 2009; 113:1786–93. [PubMed: 19029439]

McCoy AJ, Grosse-Kunstleve RW, Adams PD, Winn MD, Storoni LC, Read RJ. Phaser crystallographic software. J Appl Crystallogr. 2007; 40:658–674. [PubMed: 19461840]

McLellan JS, Yao S, Zheng X, Geisbrecht BV, Ghirlando R, Beachy PA, Leahy DJ. Structure of a heparin-dependent complex of Hedgehog and Ihog. Proc Natl Acad Sci U S A. 2006; 103:17208–13. [PubMed: 17077139]

Meyerhardt JA, Look AT, Bigner SH, Fearon ER. Identification and characterization of neogenin, a DCC-related gene. Oncogene. 1997; 14:1129–36. [PubMed: 9121761]

Otwinowski, Z.; Minor, W. Methods in Enzymology. Academic Press; 1997. Processing of X-ray Diffraction Data Collected in Oscillation Mode; p. 307-326.

Rajagopalan S, Deitinghoff L, Davis D, Conrad S, Skutella T, Chedotal A, Mueller BK, Strittmatter SM. Neogenin mediates the action of repulsive guidance molecule. Nat Cell Biol. 2004; 6:756–62. [PubMed: 15258590]

Saff EB, Kuijlaars ABJ. Distributing many points on a sphere. Mathematical Intelligencer. 1997; 19:5–11.

Schmidtmer J, Engelkamp D. Isolation and expression pattern of three mouse homologues of chick Rgm. Gene Expr Patterns. 2004; 4:105–10. [PubMed: 14678836]

Su XD, Gastinel LN, Vaughn DE, Faye I, Poon P, Bjorkman PJ. Crystal structure of hemolin: a horseshoe shape with implications for homophilic adhesion. Science. 1998; 281:991–5. [PubMed: 9703515]

Vielmetter J, Kayyem JF, Roman JM, Dreyer WJ. Neogenin, an Avian Cell-Surface Protein Expressed during Terminal Neuronal Differentiation, Is Closely-Related to the Human Tumor-Suppressor Molecule Deleted in Colorectal-Cancer. Journal of Cell Biology. 1994; 127:2009–2020. [PubMed: 7806578]

Vielmetter J, Chen XN, Miskevich F, Lane RP, Yamakawa K, Korenberg JR, Dreyer WJ. Molecular characterization of human neogenin, a DCC-related protein, and the mapping of its gene (NEO1) to chromosomal position 15q22.3-q23. Genomics. 1997; 41:414–21. [PubMed: 9169140]

Wilson NH, Key B. Neogenin interacts with RGMa and netrin-1 to guide axons within the embryonic vertebrate forebrain. Dev Biol. 2006; 296:485–98. [PubMed: 16836993]

Wilson NH, Key B. Neogenin: one receptor, many functions. Int J Biochem Cell Biol. 2007; 39:874–8. [PubMed: 17137827]

Yang F, West AP Jr. Allendorph GP, Choe S, Bjorkman PJ. Neogenin interacts with hemojuvelin through its two membrane-proximal fibronectin type III domains. Biochemistry. 2008; 47:4237–45. [PubMed: 18335997]

Zhang AS, West AP Jr. Wyman AE, Bjorkman PJ, Enns CA. Interaction of hemojuvelin with neogenin results in iron accumulation in human embryonic kidney 293 cells. J Biol Chem. 2005; 280:33885–94. [PubMed: 16103117]

Zhang AS, Yang F, Wang J, Tsukamoto H, Enns CA. Hemojuvelin-neogenin interaction is required for bone morphogenic protein-4-induced hepcidin expression. J Biol Chem. 2009; 284:22580–9. [PubMed: 19564337]

Zhang AS, Anderson SA, Meyers KR, Hernandez C, Eisenstein RS, Enns CA. Evidence that inhibition of hemojuvelin shedding in response to iron is mediated through neogenin. J Biol Chem. 2007; 282:12547–56. [PubMed: 17331953]

Zhang AS, Yang F, Meyer K, Hernandez C, Chapman-Arvedson T, Bjorkman PJ, Enns CA. Neogenin-mediated hemojuvelin shedding occurs after hemojuvelin traffics to the plasma membrane. J Biol Chem. 2008; 283:17494–502. [PubMed: 18445598]

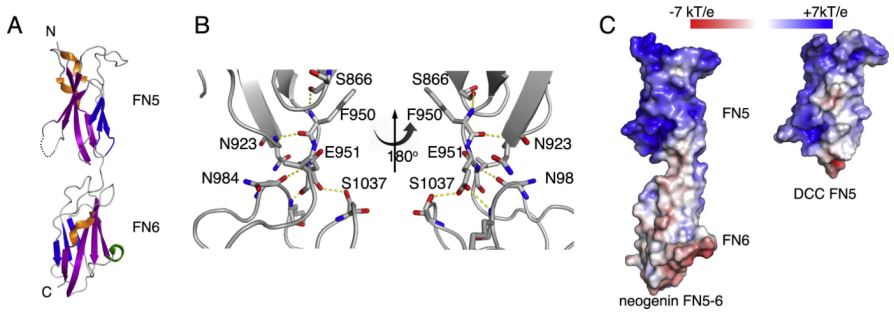

Figure 1.

Crystal structure of neogenin FN5-6. (A) Ribbon diagram of the neogenin FN5-6 structure. N- and C-termini are labeled. β-strands A, B, and E are blue, strands C, C', F, and G are purple, polyproline helices are orange and a 3_{10} helix is green. A dashed line indicates the disordered loop missing in the final model. (B) Hydrogen bonding (dotted yellow lines) at the inter-domain interface. Oxygen atoms are red and nitrogen atoms are blue in the highlighted side-chains. (C) Electrostatic potential surfaces for neogenin FN5-6 and DCC FN5 (PDB code 2EDD). Electrostatic potentials were calculated using the APBS tool (Baker et al., 2001) and plotted from −7 kT/e (red, electronegative) to +7 kT/e (blue, electropositive).

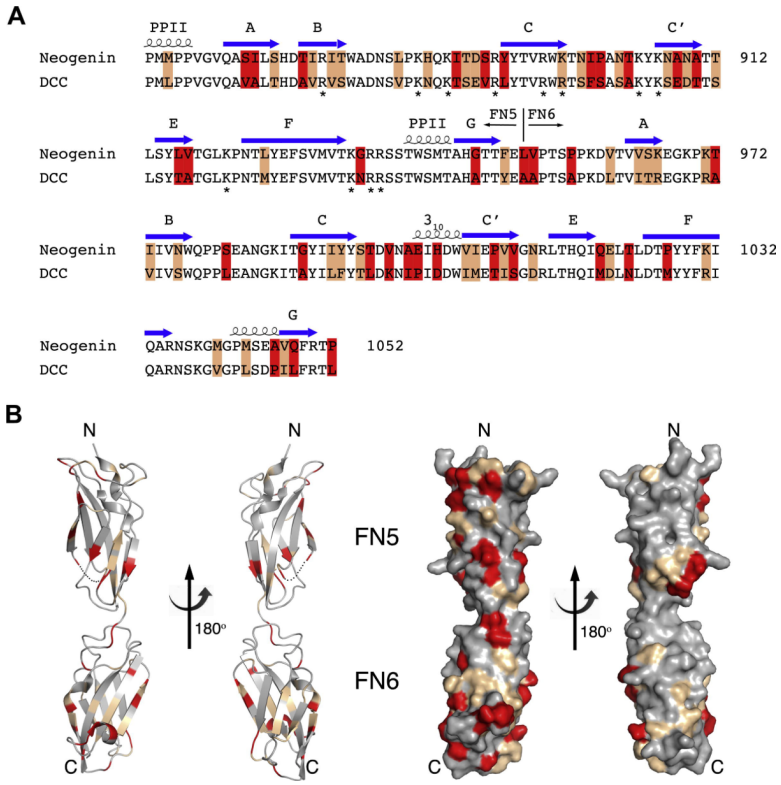

Figure 2.

Structure-based sequence alignment of the FN5-6 regions of human neogenin and DCC. (A) Sequence alignment of neogenin FN5-6 with the counterpart region of DCC (GenBank accession codes AAC51287 and NP_005206). Secondary structure elements determined from the structure of neogenin FN5-6 are indicated above the sequences (arrows for β-strands and springs for helices). Non-conserved residues representing potential interaction sites with hemojuvelin are highlighted in red, residues that are similar but not identical are highlighted in light brown, and conserved residues are not highlighted, with the exception of conserved positively-charged residues in FN5, which are marked with an asterisk. (B) Ribbon diagram and surface representation of neogenin FN5-6 using the color scheme from panel A to highlight non-conserved regions (red) as potential binding sites for hemojuvelin.

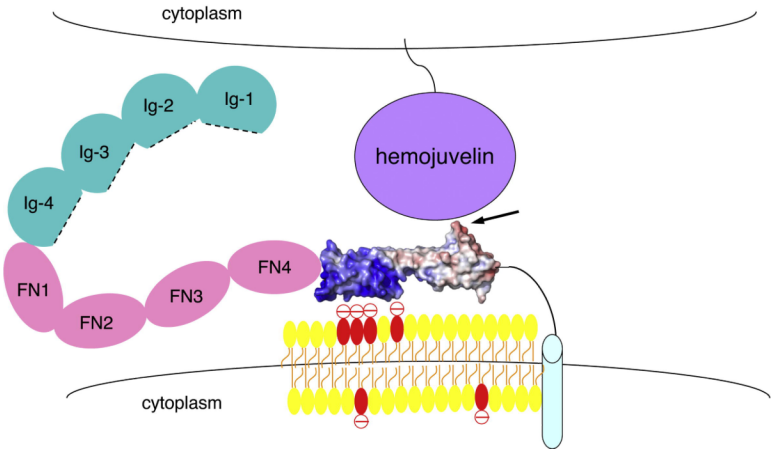

Figure 3.

Hypothetical model for how interactions between neogenin FN5 and negatively-charged phospholipids on the surface of the neogenin-expressing cell could facilitate interactions between hemojuvelin on the surface of another cell and the hemojuvelin-binding site on neogenin FN6. The neogenin FN5-6 structure is shown as in Figure 1C as an electrostatic surface, with the highly positive FN5 domain (blue) interacting with negatively-charged lipids (red). The remaining domains of neogenin are represented as cyan (Ig-like domains) and pink shapes (FNIII domains). A black arrow points to the 3_{10} helix within the potential hemojuvelin binding site in the FN6 domain.

Table 1

Data collection and refinement statistics

Unit cell	**Space group**	**$C222_1$**
Cell dimensions	a, b, c (Å)	52.6, 112.9, 80.9
Data collection		
	Resolution (Å)	32.8-1.8 (1.86-1.80)
	$^{a}R_{merge}$ (%)	5.9 (37.8)
	Completeness	99.3 (98.2)
	I/σI	28.2 (4.2)
	Mean redundancy	3.8 (3.7)
	No. of unique/total reflections	22544/85823
Refinement statistics		
	Resolution (Å)	32.8-1.8
	No. reflections used	22481
	No. reflections in working/test set	21391/1090
	R_{cryst}/ R_{free} (%)	20.0/23.4
No. Atoms (B factor: Å^2)		
	Protein	1577 (23.75)
	Water	293 (35.49)
RMS deviations		
	Bond length (Å)	0.010
	Angle (°)	1.596
Ramachandran plot (%)		
	Preferred	187 (96.4%)
	Allowed	7 (3.6%)
	Outlier	0 (0.0%)

$^{a}R_{merge}$ (%) = 100 × ∑|I−<I>|/∑I, where I is the integrated intensity of a given reflection. Numbers in parentheses are statistics for the highest resolution shell.

$^{b}R_{cryst}$ (%) = 100 × ∑ |F_{obs}−F_{calc}|/∑F_{obs}, where the F_{obs} and F_{calc} are the observed and calculated structure factor amplitudes for all reflections in the working set.

$^{b}R_{free}$ was calculated as described for R_{cryst} but summed over the 5% of reflections that were not included in the refinement.

Table 2

Interdomain tilt, rotation angles and buried surface area

	PDB code	Tilt (°)*	Rotation (°)	Buried surface area (Å^2) ***
neogenin FN5-6	TBD	169	148	501
neuroglian FN1-2	1CFB	104	172	308
fibronectin FN7-8	1FNF	129	112	601
fibronectin FN8-9	1FNF	134	158	540
fibronectin FN9-10	1FNF	157	42	338
β4 integrin	1QG3	155;156**	150;153	392
NCAM FN1-2	2VKW	57;59	140;140	530
NCAM2 FN1-2	2JLL	122	89	280
Ihog FN1-2	2IBB	42	137	1170

* Tilt angle (defined as the angle between the long axes of two adjacent domains) was calculated using the program Dom_angle (Su et al., 1998). Rotation angle (kappa in polar coordinates) was calculated using COOT by superimposing the secondary structures of the two domains.

** Two angles were calculated due to slight conformational differences between two copies of the same molecule.

*** Total buried surface areas were calculated using CCP4 program AREAIMOL and a 1.4 Å probe.